Reaction Dynamics of H + O_2 at 1.6 eV Collision Energy

Michael J. Bronikowski, Rong Zhang,
David J. Rakestraw*, and Richard N. Zare

Department of Chemistry
Stanford University
Stanford, California 94305
U.S.A.

*Present Address: Division 8362
Sandia National Laboratory
P. O. Box 969
Livermore, CA 94551-0969

Abstract

The hot H atom reaction, H + O_2 --> OH + O, has been studied at a center of mass collision energy of 1.6 eV. H atoms were generated by 266 nm photolysis of HI in a mixture of HI and O_2 at 293 K. The OH product was probed by laser induced fluorescence and the nascent OH vibrational, rotational, and fine structure distributions were determined. The OH(v=0)/OH(v=1) vibrational branching ratio was measured to be 1.72 ± 0.09. Our data suggest that the H + O_2 reaction at this collision energy proceeds via two competing mechanisms: reaction involving a long-lived complex and direct reaction.

1. Introduction

The endothermic reaction

$$H(^2S) + O_2(^3\Sigma_g^-) \rightarrow OH(^2\Pi) + O(^3P) \quad \Delta H = 16.6 \text{ kcal/mole} \qquad (1)$$

is the basic chain-branching step in H_2/O_2 combustion. The value of its rate coefficient is of considerable practical importance because it controls flame propagation and ignition. Moreover, reaction (1) is relevant to hydrocarbon combustion: 80% of the O_2 consumption in a typical hydrocarbon-air stoichiometric flame at atmospheric pressure occurs via this reaction [1]. Many kinetic studies of reaction (1) have been carried out over a wide range of temperatures [2-6]. However, there is considerable spread (about a factor of 6) in the values of the rate coefficient measured at flame temperatures in excess of 2000 K. In addition, the scatter in the data makes it difficult to ascertain the temperature dependence of the rate coefficient.

One possible way to decide between these conflicting measurements is to compare them to dynamical calculations on an ab initio surface. A global ab initio surface for the ground electronic state ($^2A''$) of this system has been constructed by Melius and Blint [7], and an improved surface in the region of the minimum energy path has been developed by Walch et al. [8] (It should be noted that the HO_2 radical does have a low-lying electronic excited state of $^2A'$ symmetry, 0.87 eV above the ground state [9,10], which is

energetically accessible in this reaction.) Kleinermanns and Schinke [11] have performed classical trajectory calculations on the Melius-Blint surface at H atom collision energies of 1.2 eV, 2.6 eV and 3.9 eV. Their principal result was that the specificity of initial conditions needed for reaction increases as the collision energy increases (e.g., the range of impact parameters leading to reaction becomes progressively narrower with increasing energy). This leads to decreasing reaction cross section and increasingly non-statistical OH product state distributions (rotational distributions narrowly peaked at high N) as the H atom energy is increased. To test the validity of such potential energy surfaces and dynamical calculations, it is desirable to compare the predictions of the calculations with reliable experimental state distributions of the reaction products at a given center-of-mass collision energy.

Kleinermanns, Wolfrum, and Linnebach [12,13] have investigated the OH product distribution for the H + O_2 reaction. They obtained hot H atoms by photodissociating HBr and HI at 193 and 248 nm, respectively, and probed the nascent rotational and fine structure populations of the OH product using laser induced fluorescence (LIF). However, their studies had several shortcomings: dissociation of HI at 248 nm yields I atoms in two spin-orbit states ($^2P_{3/2}$ and $^2P_{1/2}$, in the ratio 0.75 : 1 [14]), which differ in energy by about 0.95 eV. These two dissociation channels correspond to two different possible center-of-mass H atom energies, 1.9 eV and 1.0 eV, respectively. Similarly, dissociation of HBr at 193 nm yields center-of-mass H atom energies of 2.6 and 2.1 eV, in the ratio 5.7 : 1 [14]. In each case, both the higher and lower H atom energies are greater than the H + O_2 energy barrier (approximately equal to the endothermicity [8], 0.72 eV [15]). Consequently, both H atoms can react with O_2 to form OH products. Thus, the OH product distribution is the sum of contributions from reactions at two different energies, which cannot be separated experimentally.

Another shortcoming of previous studies is that, although OH vibrational excitation was observed, no OH(v=1) rotational distributions were reported, and very little information about the OH(v=0)/OH(v=1) vibrational branching ratio is given. This ratio is

not reported for the 1.9 or 1.0 eV H atom distributions, and although an estimate of OH(v=1)/OH(v=0) = 0.47 ± 0.15 is given in the 2.6 eV case, this number was not measured experimentally, but rather was estimated by extrapolation of experimental data using a surprisal analysis. This was necessary because many energetically accessible high N OH states could not be probed by LIF because of predissociation of the excited OH A state.

Experiments at lower photolysis energies would avoid both the formation of reactive H atoms at two energies and the population of OH(v,N) states difficult to probe by LIF. Accordingly, we undertook the study of H + O_2 at an H atom center-of-mass collision energy of 1.6 eV, which was obtained by photodissociation of HI at 266 nm. At this wavelength, I($^2P_{3/2}$) and I($^2P_{1/2}$) are produced in the ratio 1.8 : 1 [16], corresponding to H atom energies of 1.55 and 0.62 eV, respectively. We estimate total reaction energies of 1.60 eV and 0.69 eV, including the energy contribution from the O_2 and HI thermal distributions (see, e.g., Marinero, Rettner, and Zare [17]). The 0.69 eV energy is less than the reaction endothermicity of 0.72 eV, so it was expected that contribution to the OH state distribution by the slower H atom would be minor. Also, our experimental conditions are at lower probe laser power and reduced values of PΔt (the product of total reactant pressure P times the time delay Δt between photolysis and probe pulses) than previously reported, making our derived distributions subject to less error from saturation or collisional relaxation.

Our purpose in performing this study is to measure the complete rotational, vibrational, and fine structure distributions of the OH product for the H + O_2 reaction at 1.6 eV. In particular, we wish to determine the OH(v=1) distribution and to make an accurate measure of the OH(v=0)/OH(v=1) vibrational branching ratio.

2. Experimental

Our experimental method involves generation of high kinetic energy ("hot") H atoms by laser photolysis of HI. These hot H atoms are allowed to react with room temperature O_2 to form O and OH, the latter of which is detected by laser induced fluorescence (A-X

transition, 280-360 nm). Our experimental apparatus has been described in detail elsewhere [18]. HI (Matheson, >98% purity) and O_2 (Liquid Carbonic, 99.9%) in equal concentrations were flowed through a stainless steel reaction chamber, which was exhausted by a partially throttled diffusion pump equipped with a liquid-nitrogen-cooled baffle.

Our pulsed pump and probe lasers were set up in counter-propagating beam geometry, with both lasers operating at 20 Hz. The photolysis (pump) beam, 3 mm in diameter, consisted of 266 nm light (7 mJ/pulse) from the fourth harmonic of an Nd:YAG laser (Quantel YG581-10). The UV probe beam used to excite OH consisted of the doubled output of an Nd:YAG laser (Quanta Ray DCR-2A) pumped dye laser (Quantel TDL-50, bandwidth 0.2 cm^{-1}). This beam (8 mm in diameter) was aligned to completely overlap the pump beam at the center of the reaction chamber, to insure detection of all nascent OH produced in the short time delays of our experiments (100 ns). The probe laser pulse energy was about 10 μJ per pulse, which we found to be sufficiently low to avoid saturation of the OH A-X transition.

Fluorescence was detected in the vertical direction, perpendicular to the common axis of the laser beams, by a photomultiplier tube (Centronix 4283/81). Phototube signals were recorded with a gated integrator using a 1.5 μs gate (about twice the OH A-state lifetime) delayed about 20 ns from the probe pulse to distinguish fluorescence from scattered laser light. Signals were digitized (Lecroy 2249SG ADC, CAMAC modular data bus) and stored and analyzed on a microcomputer (IBM PC-XT).

In performing our experiments, we took special care to insure that the OH state populations which we observed were in fact the nascent populations, free from any collisional relaxation or line saturation. The rate of collisional relaxation depends on the product of total reactant pressure times the time delay between the pump and probe pulses ($P\Delta t$). We found that the product distribution was free from relaxation (to within experimental error) for $P\Delta t < 5 \times 10^{-9}$ Torr sec., and we took all our data at $P\Delta t = 3 \times 10^{-9}$ Torr sec.

Additional experiments showed that quenching of the OH $A^2\Sigma^+$ state was not important at the pressures we used (25 mTorr).

The probe laser was scanned in a series of runs from 306 nm to 323 nm. This wavelength range was appropriate to pump both the (0,0) and (1,1) bands of the OH A-X transition. Fluorescence observed on the (0,0) and (1,1) bands was used to calculate the OH(v=0,N) and OH(v=1,N) relative populations, while (1,0) fluorescence (observed with a separate filter) was used to confirm the OH(v=1) relative populations. Data were collected on all six main spectroscopic branches for all observed rotational levels of both vibrational states.

The normalized integrated line intensities were divided by the Einstein B coefficients [19] and a calculated filter transmission function to give relative populations. Populations calculated from P and R lines generally agreed to within 10% after normalization (these two lines probe the same Λ-doublet level). Populations of this Λ-doublet were obtained by averaging the relative populations calculated from the P and R lines.

3. Results and Discussion

Figure 1 shows a segment of the OH LIF spectrum, taken under typical experimental conditions, in the region of the OH(v=1) R_1 and R_2 bandheads. Also present in this region are several strong P and Q lines of OH(v=0). Spectra such as this one, where v=0 and v=1 data are collected together under identical experimental conditions, allow us to compare directly the derived OH(v=0,N) and OH(v=1,N) populations.

Figure 2 shows the measured rotational distributions of all fine structure components of both OH(v=0) and OH(v=1). Due to spectral congestion, several lines in the OH spectrum could not be observed; data on these OH(v,N) states are not included in the figure. OH(v=0,N) levels are populated up to N = 20 (the highest N permitted by energetic limits) with maximum population at N = 14-15. For OH(v=1,N), the maximum occurs at N = 9-10, with rotational levels populated as high as N = 14, the highest energetically allowed N for

v=1. For both vibrational states, we observe that the lower energy OH($^2\Pi_{3/2}$) spin-orbit component is more populated than the higher energy OH($^2\Pi_{1/2}$) component, while for both spin-orbit components, the A' Λ-doublet level (unpaired electron orbital lobes lie in the plane of rotation of the molecule) has more population than the A" Λ-doublet level (unpaired electron orbital lobes perpendicular to the plane of rotation [20]). The trend in the N-dependent Λ-doublet ratios (to be discussed in detail below) is apparent from this figure: the two levels are almost equally populated at low N, but the A'/A" ratio increases as N increases, reaching a maximum value of about 2 for high N.

One interesting aspect of the OH(v=0) data is the presence of a secondary maximum at N = 1 in both of the OH($^2\Pi_{3/2}$) Λ-doublet distributions, with the populations decreasing with increasing N until about N = 6. As described in section 2, we are confident that we are not observing collisional relaxation of the OH product. We attribute this excess low-N population to reaction of O_2 with the slow H atom associated with the spin-orbit excited iodine atom in the photolysis of HI. Because the slow H atom has an energy of 0.69 eV, which is less than the reaction endothermicity of 0.72 eV, this reaction must be coming entirely from the high-energy Boltzmann tail of the translational and rotational energy distributions of HI and O_2.

To estimate the contribution of the slow H atom to the total OH(v=0) population, we used a surprisal analysis similar to that used by Kleinermanns and Linnebach [13]. For each spin-orbit component, a surprisal plot of rotational state population (summed over Λ-doublets) was observed to be linear in the range $8 < N < 14$. This region of linear surprisal plot was assumed to contain states populated only by reaction of O_2 with the fast H atom. A straight line was fit to the points N = 9-13 and was extended with the same slope to lower N to obtain the contributions from the high energy H atom to these states. The differences between these calculated populations and the observed populations was taken to be the contribution from the slow H atom. The sum (over the low N states) of this contribution was our estimate of the contribution from the low energy H atom to the total OH(v=0) product observed. Using this

method, we estimate the relative contribution of the 0.69 eV H atom to be 9.4% ± 3.6% of the total OH(v=0) population, which corresponds to 6.1% ± 2.3% of the total observed OH product. Subtracting this contribution from the total OH(v=0) population, we obtain the vibrational branching ratio for reaction of 1.6 eV H atoms with O_2:

$$OH(v=0)/OH(v=1) = 1.72 \pm 0.09 \qquad (2)$$

The uncertainty given above includes a contribution of 0.06 from the estimated error in the surprisal extrapolation.

We can also gain insight by examining the N-dependent ratios of the populations of the various fine structure components. Figure 3 shows the ratios of the populations of the two spin-orbit components (summed over both Λ-doublets, divided by the total angular momentum degeneracy, 2J+1) for v=0 and v=1. For a statistical distribution, we would expect a $OH(^2\Pi_{3/2})/OH(^2\Pi_{1/2})$ ratio of 1.0 for the same J value. In both vibrational states there is a marked N-dependent preference for the lower energy $OH(^2\Pi_{3/2})$ spin-orbit component. For N > 5, the ratio is approximately constant at 1.22 ± 0.12 for v=0 and 1.34 ± 0.07 for v=1. The v=0 ratio takes on higher values at low N, up to 2.1 for N = 0,1. It is at these low values of N that the 0.69 eV H atom contributes significantly to the OH population, and thus it is apparent that this low energy H atom has a higher propensity than the 1.6 eV H atom to populate the $OH(^2\Pi_{3/2})$ state.

One possible explanation for the observed spin-orbit ratios is that the two different OH spin-orbit components correlate with different spin-orbit components of the product $O(^3P_{2,1,0})$. The spin-orbit ratio we observe might represent a preference for reaction on one electronic fine structure surface over another (a surface leading to the $OH(^2\Pi_{1/2})$ product). Further work will be needed to investigate this question more fully.

Figure 4 shows the Λ-doublet ratios for $OH(^2\Pi_{3/2})$, v=0 and 1, respectively (the results for the $^2\Pi_{1/2}$ component are similar). These plots indicate a preference for the A' component which increases with increasing N. This preference is consistent with a

planar reaction mechanism (that is, a reaction which occurs preferentially for H-O_2 collisions with the H atom velocity vector in the plane of the three atoms), as we now show. In the following discussion, the term "plane" used in the expressions in-plane and out-of-plane refers to the instantaneous plane described by the three atoms.

As the HO_2 complex falls apart to form OH and O, the breaking O-O bond correlates asymptotically with the singly occupied OH $p\pi$ orbital whose lobes point along the line of the broken bond, i.e. lie in the plane of the atoms. The forces that break the bond are necessarily in-plane forces, and so exert a torque on the OH perpendicular to this plane. This results in a component of the OH angular momentum N perpendicular to the plane. An H-O_2 collision whose H atom velocity is in-plane will give an HO_2 complex with angular momentum perpendicular to the plane, which can contribute to the perpendicular component of N upon dissociation. On the other hand, H-O_2 collisions with the H atom velocity vector lying out-of-plane will result in large components of HO_2 angular momentum in the plane of the three atoms (i.e., out-of-plane rotation of the HO_2 complex, with the plane of the atoms tumbling in space), which will in turn give a large in-plane component of N upon dissociation of the complex. An in-plane reaction mechanism would therefore result in N perpendicular to the OH $p\pi$ lobes (A' Λ-doublet), whereas an out-of-plane mechanism would give N parallel to the OH $p\pi$ lobes (A" Λ-doublet). Our observed preference for the A' Λ-doublet thus indicates a preference for an in-plane mechanism in the reaction of H with O_2 at 1.6 eV.

Notice that the A'/A" ratio approaches unity with decreasing N. This behavior does not imply that an out-of-plane mechanism becomes important with decreasing N. Rather, it arises because as N decreases, the OH radical more nearly follows Hund's case (a) coupling: the rotational quantum number N and the plane of rotation of the molecule are not well defined, and so the distinction between the unpaired electron orbitals lying in-plane and out-of-plane loses its meaning. The two Λ-doublet levels remain as distinct levels, but at low N they no longer correspond to in-plane and out-of-plane

orbital orientations and so no longer serve as indicators of the mechanism by which reaction occurred. We see that the A'/A" ratio approaches unity (which we would expect in a statistical distribution, since the OH Λ-doublet splitting is very small, typically a few wave numbers). This suggests that there are no dynamical processes other than the reaction mechanisms described above which influence the Λ-doublet ratio at low N.

The Λ-doublet ratio increases with increasing N, leveling off at high N to a value of 2.06 ± 0.11 for v=0 and 1.93 ± 0.09 for v=1. Kleinermanns and Linnebach [13] reported a maximum A'/A" ratio for OH(v=0) of 5.9 ± 1.0 at an H atom energy of 2.6 eV, 2.6 ± 0.2 at 1.9 eV, and 1.7 ± 0.2 at 1.0 eV. They concluded that a non-planar reaction pathway becomes more important in the H + O_2 reaction as the collision energy is lowered. Our observation of A'/A" = 2.06 for OH(v=0) at 1.6 eV is consistent with these measurements and this interpretation.

The trajectory calculations of Kleinermanns and Schinke [11] suggest that at low collision energies (1.2 eV), the H + O_2 reaction proceeds via a long-lived complex which yields a statistical OH product distribution. As the collision energy increases (2.6 eV and 3.9 eV) the reaction becomes more direct, with increasingly non-statistical rotational distributions peaked at high N. We used the phase space theory of Pechukas, Light, and Rankin [21] to calculate the statistical populations of the product OH(v,N) states and compared these to our experimental results. Figure 5 shows plots of the experimental and calculated results, normalized to have the same area (same total population), for OH(v=0) and OH(v=1). For OH(v=0), we compare only those rotational states for which we are confident that the experimental populations have negligible contribution from the 0.69 eV H atom. The experimental populations have been summed over the spin-orbit components and Λ-doublet levels because the statistical theory does not take into account the possibility of different fine structure states. The agreement between theory and experiment seems reasonable for v=1. However, the v=0 experimental distribution is clearly non-statistical, with more population in the high N states than the calculated distribution. The

phase space calculations also predicted an OH(v=0)/OH(v=1) ratio of 1.99. This ratio was observed to be somewhat sensitive to our choice of reaction parameters such as total energy and O-OH dispersion (van der Waals) coefficient. Therefore, we feel that the calculated vibrational ratio agrees reasonably well with our experimental value of 1.72 ± 0.09.

One possible explanation of these results is as follows: our experimental energy of 1.6 eV lies between the low energy (1.2 eV) and high energy (> 2.6 eV) regimes of reference 10. It may be that at this energy we observe a competition between two mechanisms: a long-lived complex which leads tc a statistical product state distribution, and a direct reaction which for the OH(v=0) channel favors high rotational levels. This might account for the nearly statistical nature of much of our experimental distribution (vibrational ratio and OH(v=1) distribution), and the non-statistical component of the OH(v=0) distribution. Although the rotational-vibrational distribution has a large degree of statistical character, the reaction is clearly not completely statistical in nature, as can be seen, for example, from the non-statistical fine structure distributions. Dynamics still play an important role in the H + O_2 reaction at this energy.

Acknowledgement

We thank W. J. van der Zande for many useful discussions in the preparation of this paper. MJB thanks the National Science Foundation for a Graduate Fellowship. This work was supported by the NASA Ames Research Center under grant NAG 2-472, and by the National Science Foundation under grant NSF CHE 87-05131.

References

[1] W. C. Gardiner, Combustion Chemistry (Springer-Verlag, New York, 1984) p. 205

[2] D. L. Baulch, D. D. Drysdale, and D. G. Horne, in: Fourteenth Symposium (International) on Combustion (The Combustion Institute, Pittsburgh, 1973) p. 107

[3] G. L. Schott, Combust. Flame 21 (1973) 357

[4] C. T. Bowman, in: Fifteenth Symposium (International) on Combustion (The Combustion Institute, Pittsburgh, 1975) p. 869

[5] P. Franck and Th. Just, Ber. Bunsenges. Phys. Chem. 89 (1985) 181

[6] N. Fujii and K. S. Shin, Chem. Phys. Lett. 151 (1988) 461

[7] C. F. Melius and R. J. Blint, Chem. Phys. Lett. 64 (1979) 183

[8] S. P. Walch, C. M. Rohlfing, C. F. Melius, and C. W. Bauschlicher, J. Chem. Phys. 88 (1988) 6273

[9] K. H. Becker, E. H. Fink, P. Langen, and U. Schurath, J. Chem. Phys. 60 (1974) 4623

[10] S. R. Langhoff and R. L. Jaffe, J. Chem. Phys. 71 (1979) 1475

[11] K. Kleinermanns and R. Schinke, J. Chem. Phys. 80 (1984) 1440

[12] K. Kleinermanns and J. Wolfrum, J. Chem. Phys. 80 (1984) 1446

[13] K. Kleinermanns and E. Linnebach, J. Chem. Phys. 82 (1985) 5012

[14] G. W. Flynn and R. E. Weston, Ann. Rev. Phys. Chem. 37 (1986) 551, and references therein

[15] K. P. Huber and G. Herzberg, Molecular Spectra and Molecular Structure IV. Constants of Diatomic Molecules (Van Nostrand Reinhold Company, New York, 1974)

[16] R. D. Clear, S. J. Riley, and K. R. Wilson, J. Chem. Phys. 63 (1975) 1340

[17] E. E. Marinero, C. T. Rettner, and R. N. Zare, J. Chem. Phys. 80 (1984) 4142

[18] K. G. McKendrick, D. J. Rakestraw, and R. N. Zare, Faraday Disc. Chem. Soc. 84 (1987) 1

[19] I. L. Chidsey and D. R. Crosley, J. Quant. Spectrosc. Radiat. Transfer 23 (1980) 187

[20] M. H. Alexander et al., J. Chem. Phys. 89 (1988) 1749

[21] P. Pechukas, J. C. Light, and C. Rankin, J. Chem. Phys. 44 (1966) 794

Fig. 1. Segment of the OH A-X LIF spectrum for the OH reaction product from the reaction H + O_2 --> O + OH(v,N) at 1.6 eV collision energy. The region shown contains the R_1 and R_2 bandheads of OH(v=1), and several Q and P lines of OH(v=0). Several transitions from the R_{21} (R_1') satellite branch of OH(v=1) are also seen. These are indicated in the R_1 progression with a prime.

Fig. 2. Rotational state populations of the various fine structure components of (a) OH(v=0), and (b) OH(v=1), from the reaction of 1.6 eV H atoms with thermal O_2. Shown are N-state distributions of both Λ-doublet levels (A' and A"), for both spin-orbit components ($^2\Pi_{3/2}$ and $^2\Pi_{1/2}$) of OH(v=0) and OH(v=1).

Fig. 3. Spin-orbit ratios, OH($^2\Pi_{3/2}$)/OH($^2\Pi_{1/2}$), as a function of rotational quantum number N, for OH(v=0) and OH(v=1) from the H + O_2 reaction at 1.6 eV. The populations of the individual spin-orbit states have been summed over both Λ-doublets and divided by the degeneracy, 2J+1.

Fig. 4. Λ-doublet ratios, A'/A", as a function of N, for OH($^2\Pi_{3/2}$), v=0 and v=1, from the H + O_2 reaction at 1.6 eV. The results are similar for the OH($^2\Pi_{1/2}$) spin-orbit component.

Fig. 5. Comparison of the measured OH(v,N) distribution to a distribution calculated using phase space theory for (a) v=0, and (b) v=1. The experimental distributions have been summed over all fine structure levels. Not shown are the (v=0, N=1-6) levels which are populated significantly by the reaction of O_2 with slow H atoms.

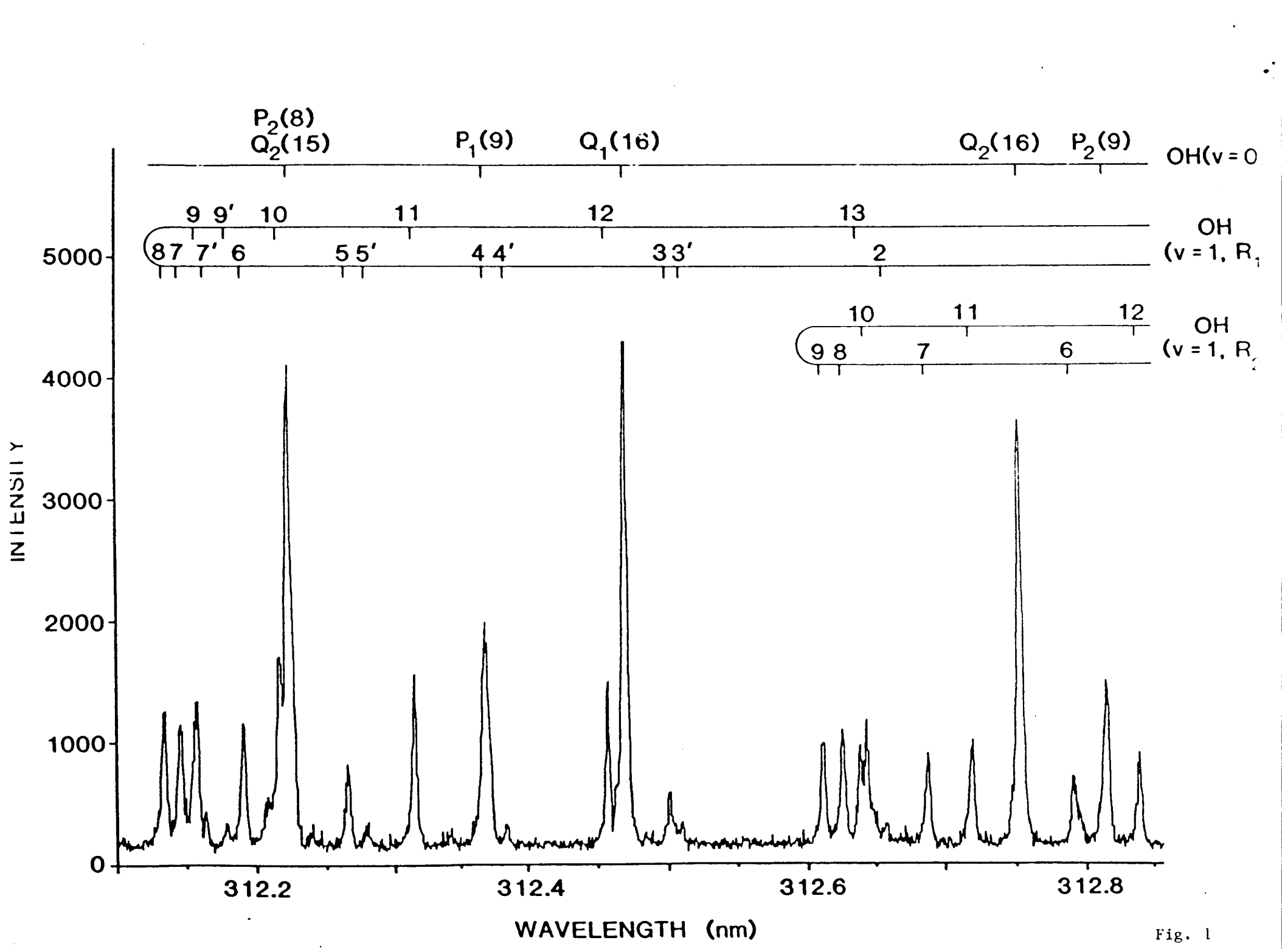
P2(8)
Q2(15)
P1(9)
Q1(16)
Q2(16)
P2(9)
OH(v = 0
9 9' 10 11 12 13
8 7 7' 6 5 5' 4 4' 3 3' 2
OH
(v = 1, R1
10 11 12
9 8 7 6
OH
(v = 1, R2
5000
4000
3000
2000
1000
0
INTENSITY
312.2
312.4
312.6
312.8
WAVELENGTH (nm)

Fig. 1

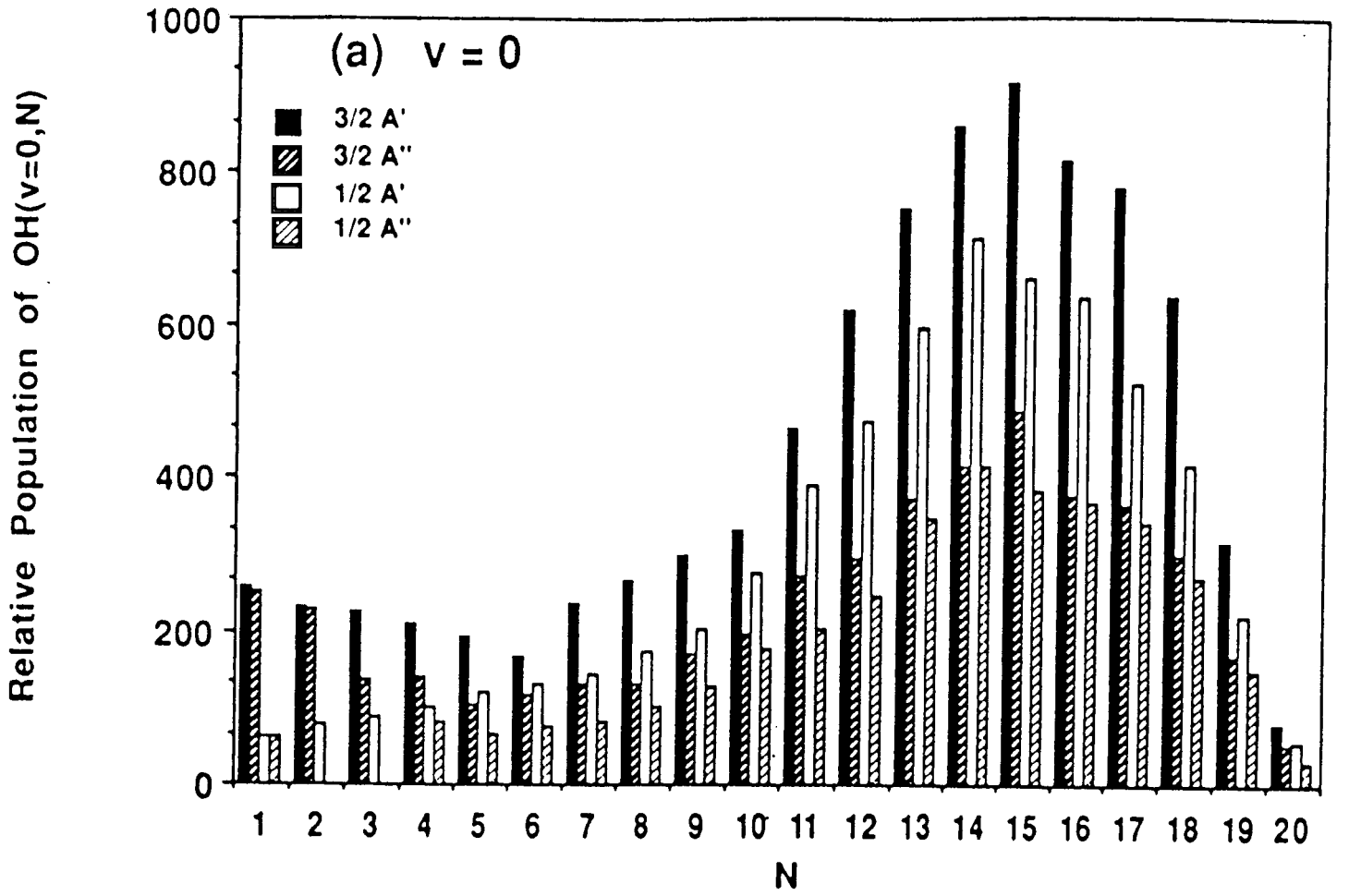
(a) v = 0
3/2 A'
3/2 A''
1/2 A'
1/2 A''
Relative Population of OH(v=0,N)
0
200
400
600
800
1000
1 2 3 4 5 6 7 8 9 10 11 12 13 14 15 16 17 18 19 20
N

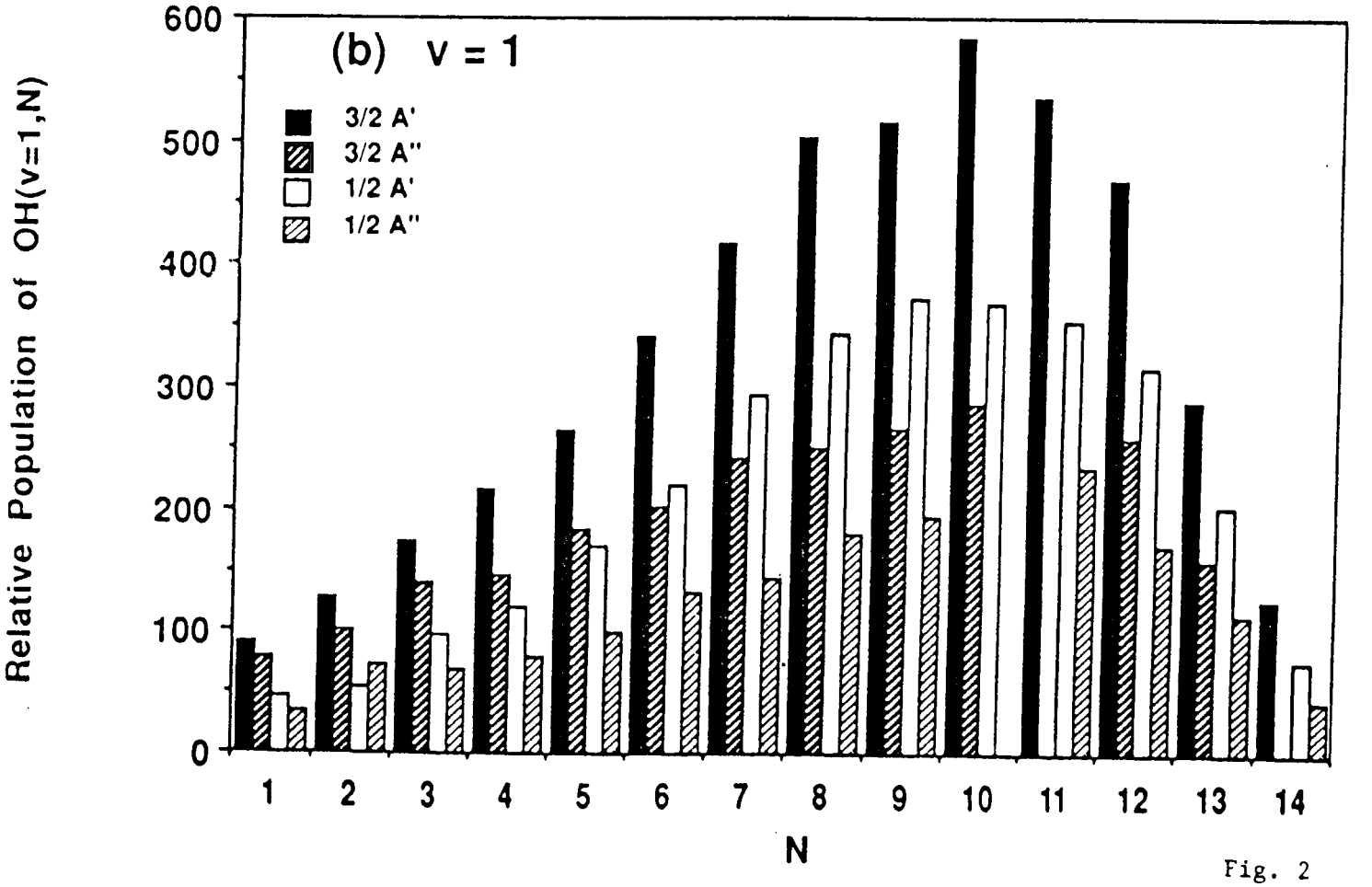
(b) v = 1
3/2 A'
3/2 A''
1/2 A'
1/2 A''
Relative Population of OH(v=1,N)
0
100
200
300
400
500
600
1 2 3 4 5 6 7 8 9 10 11 12 13 14
N

Fig. 2

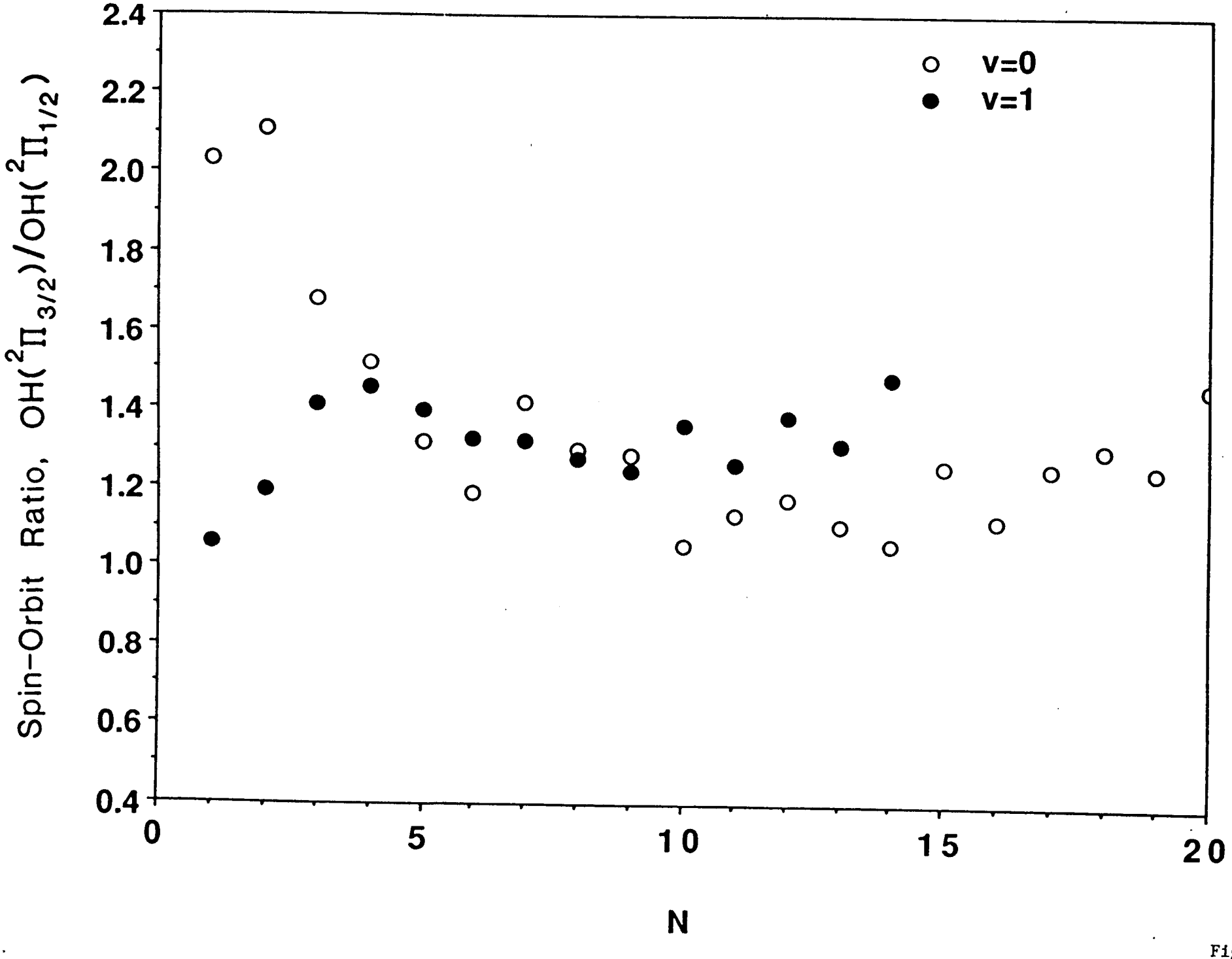
Spin-Orbit Ratio, OH($^2\Pi_{3/2}$)/OH($^2\Pi_{1/2}$)
N
v=0
v=1
2.4
2.2
2.0
1.8
1.6
1.4
1.2
1.0
0.8
0.6
0.4
0
5
10
15
20

Fig. 3

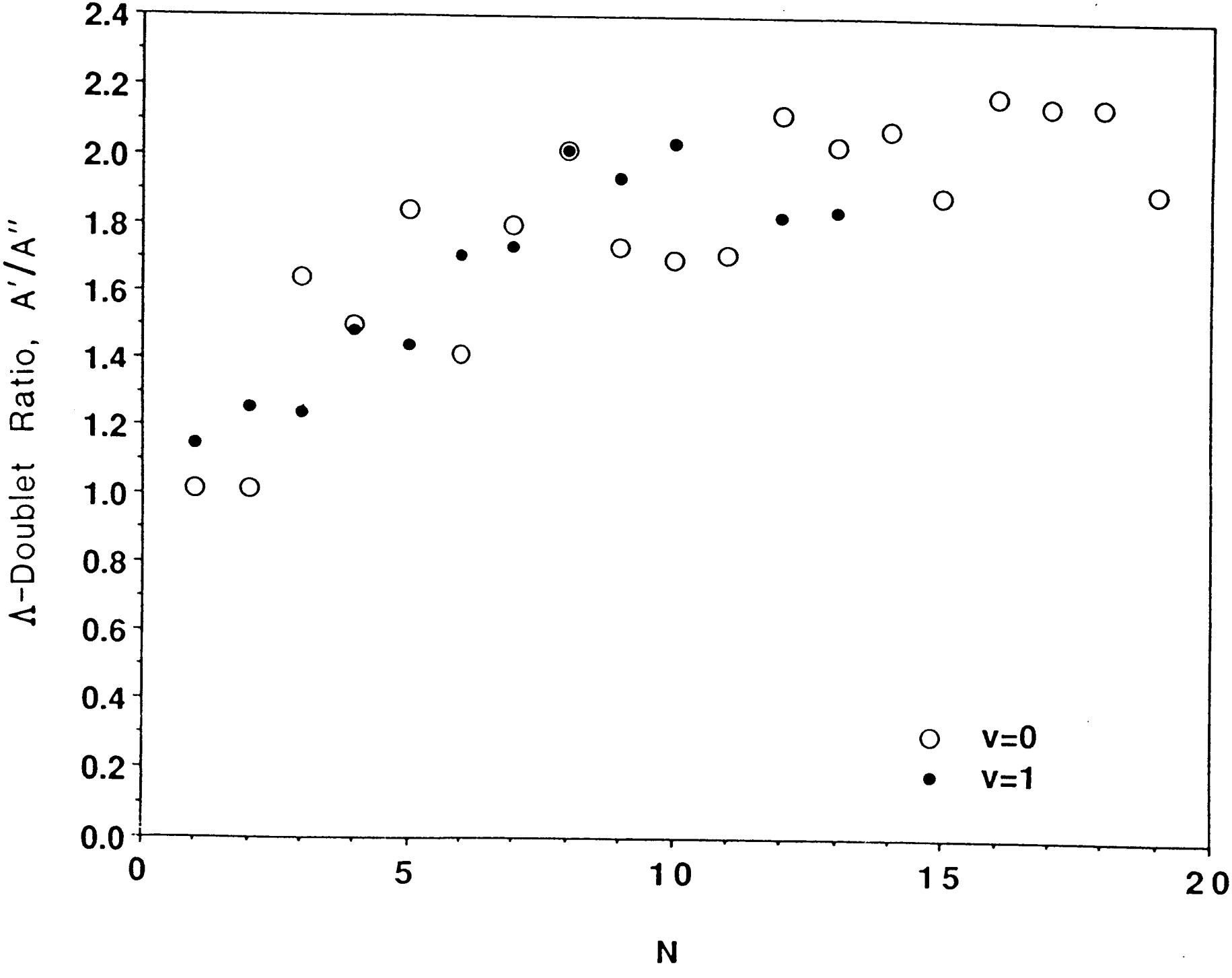
Λ-Doublet Ratio, A'/A''
2.4
2.2
2.0
1.8
1.6
1.4
1.2
1.0
0.8
0.6
0.4
0.2
0.0
0
5
10
15
20
N
v=0
v=1

Fig. 4

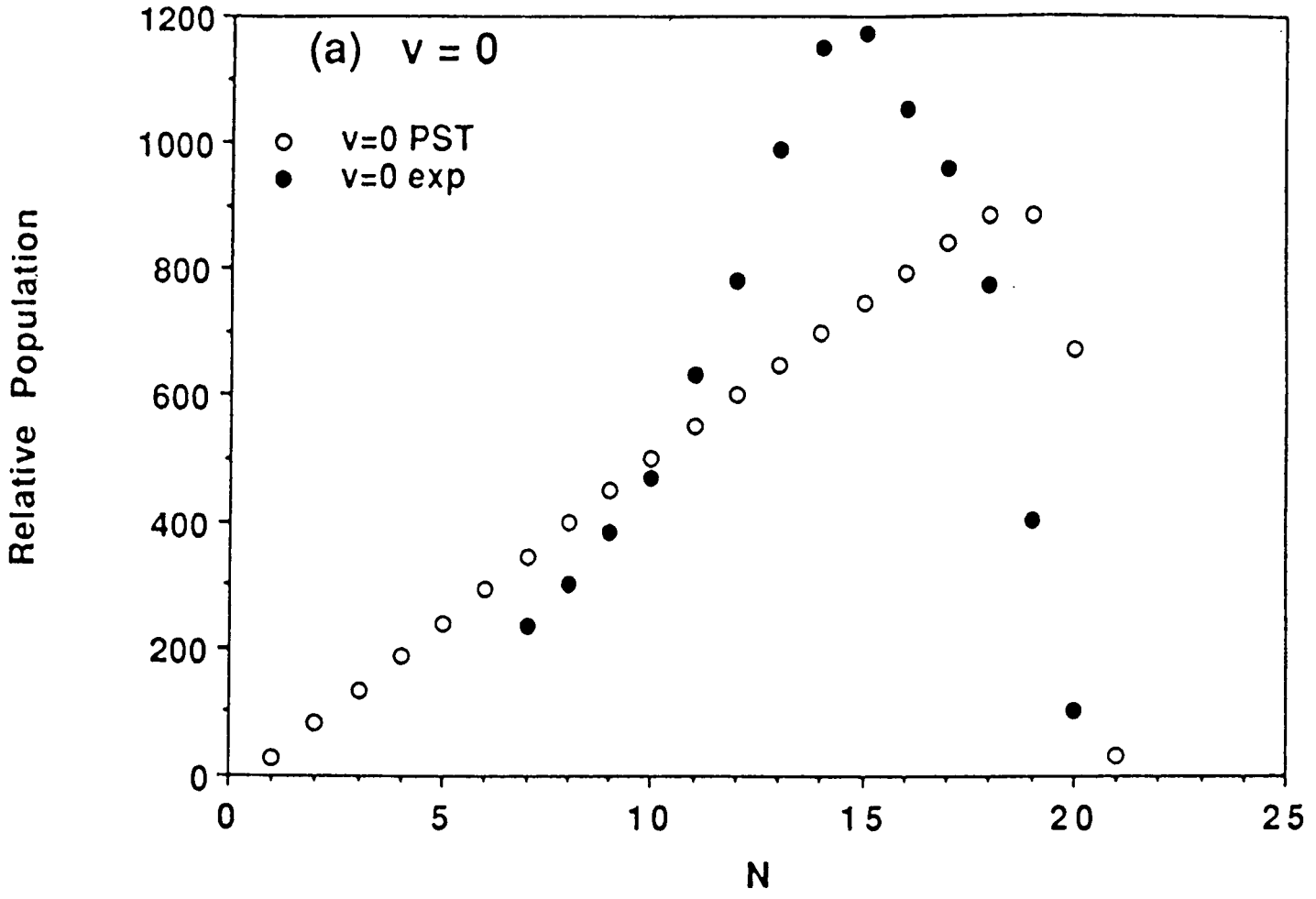
(a) v = 0
v=0 PST
v=0 exp
Relative Population
N
0
200
400
600
800
1000
1200
0
5
10
15
20
25

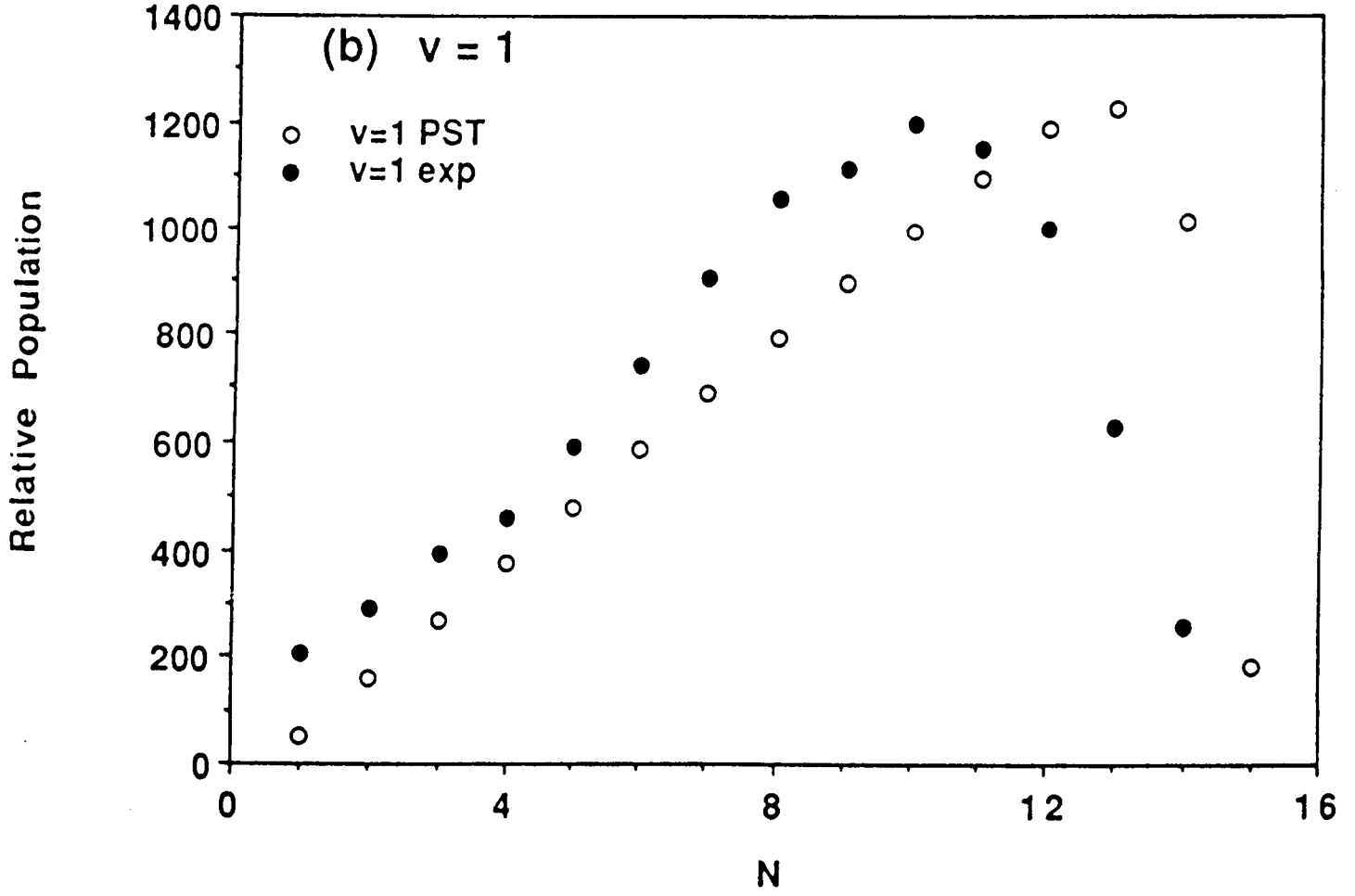
(b) v = 1
v=1 PST
v=1 exp
Relative Population
N
0
200
400
600
800
1000
1200
1400
0
4
8
12
16

Fig. 5